Astron. Astrophys. 346, 929–935 (1999)

ASTRONOMY
AND
ASTROPHYSICS

*Beppo*SAX monitoring of the "anomalous" X-ray pulsar 4U 0142+61

G.L. Israel[1,⋆], T. Oosterbroek[2], L. Angelini[3,⋆⋆], S. Campana[4,⋆], S. Mereghetti[5], A.N. Parmar[2], A. Segreto[6], L. Stella[1,⋆], J. van Paradijs[7,8], and N.E. White[3]

[1] Osservatorio Astronomico di Roma, Via Frascati 33, I-00040 Monteporzio Catone (Roma), Italy
[2] Astrophysics Division, Space Science Department of ESA, ESTEC, P.O. Box 299, 2200 AG Noordwijk, The Netherlands
[3] Laboratory for High Energy Astrophysics, Code 662, NASA – Goddard Space Flight Center, Greenbelt, MD 20771, USA
[4] Osservatorio Astronomico di Brera, Via E. Bianchi 46, I-23807 Merate (Lecco), Italy
[5] Istituto di Fisica Cosmica "G. Occhialini", CNR, Via Bassini 15, I-20133 Milano, Italy
[6] Istituto di Fisica Cosmica ed Applicazioni all'Informatica, CNR, Via U. La Malfa 153, I-90146 Palermo, Italy
[7] Astronomical Institute "Anton Pannekoek" and Center for High–Energy Astrophysics, Kruislaan 403, 1098 SJ Amsterdam, The Netherlands
[8] Physics Department, UAH, Huntsville, AL 35899, USA

Received 26 January 1999 / Accepted 30 March 1999

Abstract. The 8.7 s X-ray pulsar 4U 0142+61 was monitored by *Beppo*SAX between January 1997 and February 1998. This source belongs to the rapidly growing class of "anomalous" X-ray pulsars (AXPs) which have pulse periods in the 6–12 s range and no plausible optical, infrared or radio counterparts. The *Beppo*SAX periods measurements show that 4U 0142+61 continues its spin–down at a nearly constant rate of $\dot{\rm P} \sim 2 \times 10^{-12}$ s s^{-1}. The 0.5–10 keV pulse shape is double peaked. The phase–averaged spectrum can be described by a steep absorbed power–law ($\Gamma \sim 4$) plus a blackbody with $kT \sim 0.4$ keV.

4U 0142+61 was also detected serendipitously in a March 1996 RXTE observation pointed towards the nearby 1455 s X-ray pulsar RX J0146.9+6121. The timing analysis results are reported for this observation and the spin history of 4U 0142+61 since 1979 is discussed.

Key words: stars: evolution – stars: neutron – stars: pulsars: individual: 4U 0142+61 – X-rays: stars

1. Introduction

The properties of 4U 0142+61 (White et al. 1987) remained puzzling for a long time, owing to confusion with a nearby pulsating and transient Be/neutron star system RX J0146.9+6121 (Motch et al. 1991; Mereghetti et al. 1993). The 1–10 keV spectrum is extremely soft (power law photon index of ~ 4, White et al. 1987) and led to the initial classification of 4U 0142+61 as a possible black hole candidate. ASCA observations provide evidence for a ~ 0.4 keV blackbody component contributing ~ 40% of the 0.5–10 keV band X-ray flux (White et al. 1996). The X-ray luminosity of 4U 0142+61 has not shown substantial secular variations around an average value of $\sim 6 \times 10^{34}$ erg s^{-1} (assuming a distance of 1 kpc). Despite the small error box (5″ radius), no optical or IR counterpart has yet been identified, down to $V < 24$, $R < 22.5$, $J < 20$ and $K < 17$ (Steinle et al. 1987; White et al. 1987; Coe & Pightling 1998). These limits rule out the presence of a massive companion. Using data from the EXOSAT archive, Israel et al. (1994) discovered pulsations at 8.7 s, which were later confirmed with ROSAT (Hellier 1994). No delays in the pulse arrival times caused by orbital motion were found, with upper limits on $a_{\rm x} \sin i$ of about ~ 0.37 lt–s for orbital periods $P_{\rm orb}$ between 7 min and 12 hr (Israel et al. 1994). Tighter upper limits on the $a_{\rm x} \sin i$ (~ 0.26 lt–s for 70 s $\leq P_{\rm orb} \leq$ 2.5 days) have been recently obtained with a RXTE observation (Wilson et al. 1998). This yielded strong constraints on the orbital inclination and the mass of the possible companion star in the case of normal or helium main sequence star and giants with helium core. A white dwarf companion would be compatible both with current optical photometric and pulse arrival time limits. The EXOSAT and ROSAT period measurements, obtained in 1984 and 1993, provide a spin–down rate of $\sim 2.1 \times 10^{-12}$ s s^{-1}.

The properties of 4U 0142+61 are similar to those of a small group of "anomalous" X-ray pulsars (AXPs), with spin periods within a narrow range (6–12 s; Mereghetti & Stella 1995). Among these are 1E 2259+586, 1E 1048.1–5937, 1E 1841–045 (Vasisht & Gotthelf 1997), 1RXS 170849–400910 (Sugizaki et al. 1997) and AX J1845–045 (Torii et al. 1998; Gotthelf & Vasisht 1998).

We present here a detailed analysis of the *Beppo*SAX Narrow Field Instruments (NFIs) observations of the AXP 4U 0142+61. We confirm the presence of a blackbody spectral component in the soft X-ray spectrum as seen in the ASCA data (White et al. 1996) and in other two "anomalous" X-ray pulsars: 1E 2259+589 (Corbet et al. 1995; Parmar et al. 1998) and 1E 1048.1–5937 (Oosterbroek et al. 1998). We also present the results of pulse phase spectroscopy and the pulse period history of 4U 0142+61. We also discuss the timing analysis from

Send offprint requests to: G.L. Israel (israel@coma.mporzio.astro.it)
⋆ Affiliated to I.C.R.A.
⋆⋆ Universities Space Research Association

Table 1. 4U 0142+61 *Beppo*SAX Observation log

Start Time	Stop Time	MECS T_{exp} s	Active MECSs #	Count Rate LECS c/s	MECS c/s	Off–axis $'$	Obs
97 Jan 03 05:47	Jan 04 02:09	48226	3	1.03±0.01	1.70±0.01	5	A
97 Aug 09 23:13	Aug 10 07:38	16757	2	1.01±0.02	1.47±0.02	3	B
98 Jan 26 12:13	Jan 27 00:23	21785	2	$(4.2\pm0.4)\times10^{-2}$	0.47±0.01	20	C
98 Feb 03 09:11	Feb 04 02:37	31150	2	0.97±0.02	1.36±0.01	5	D

Note: Count rates are not vignetting corrected. Vignetting is a factor 1.10, 1.20 and 3.0 for an off–axis angle of 3, 5 and 20 arcmin, rescpectively.

Table 2. *Beppo*SAX phase averaged fit of 4U 0142+61.

Spectral Parameter	Obs. A	Obs. A[b]	Obs. D	Obs. D[b]	Obs. A[a]+D	Obs. (A+D)[b]
$N_H(10^{22}$atoms cm$^{-2})$	1.11±0.07	1.1 ±0.1	0.98±0.06	1.2±0.1	1.12±0.06	1.0±0.1
Γ	3.86±0.06	3.8 ±0.3	3.58±0.12	4.0±0.2	3.95±0.05	3.6±0.3
PL flux (erg s^{-1} cm^{-2}; 0.5–10 keV) ...	7.4×10^{-11}	6.0×10^{-11}	7.3×10^{-11}	8.4×10^{-11}	7.9×10^{-11}	7.7×10^{-11}
BB kT (keV)	0.42±0.02	0.37±0.02	0.36±0.01	0.41±0.04	0.40±0.01	0.36±0.02
BB radius (km @ 1 kpc)	1.5±0.2	2.2±0.5	2.1±0.2	1.5±0.5	1.8±0.2	2.3±0.4
BB flux (erg s^{-1} cm^{-2}; 0.5–10 keV) ...	2.9×10^{-11}	2.6×10^{-11}	4.1×10^{-11}	2.1×10^{-11}	3.0×10^{-11}	2.3×10^{-11}
χ^2/dof	440/344	214/209	309/290	203/187	455/415	283/279
L_X (10^{34} erg s^{-1} @ 1 kpc; 0.5–10 keV)	7.9	8.3	6.3	7.5	9.3	5.7

Note: Fluxes are not corrected for the interstellar absorption. Flux uncertainties are about 10%. The source luminosities were derived by setting N_H = 0.
[a] Only MECS2 and MECS3 considered.
[b] Only LECS data considered.

a serendipitous Rossi X-ray Timing Explorer (RXTE) observation of 4U 0142+61.

2. *Beppo*SAX observations

Results from the Low–Energy Concentrator Spectrometer (LECS; 0.1–10 keV; Parmar et al. 1997) and Medium–Energy Concentrator Spectrometer (MECS; 1.3–10 keV; Boella et al. 1997) on–board *Beppo*SAX are presented. The MECS consists of three identical grazing incidence telescopes with imaging gas scintillation proportional counters in their focal planes. The LECS uses an identical concentrator system as the MECS, but utilizes an ultra-thin (1.25 μm) detector entrance window and a driftless configuration to extend the low-energy response to 0.1 keV. The fields of view (FOV) of the LECS and MECS are circular with diameters of 37$'$ and 56$'$ respectively. The energy resolution of both instruments is $\simeq 8.5\sqrt{(6keV/\mathrm{E})}$% full–width half maximum (FWHM), where E is the energy.

4U 0142+61 was observed by *Beppo*SAX four times between January 1997 and February 1998 (see Table 1). One of the goals of the program was to monitor the possible X-ray flux variations on a time scale of months with two 40 ks pointings. However between the first and the subsequent observations one of the three MECS units failed (1997 May 9), and data of observations B, C and D were obtained with the remaining two MECS units. Moreover during the second and third observations *Beppo*SAX experienced pointing failures resulting in a shorter effective exposure time.

2.1. Spectral analysis

Spectra were obtained centered on the position of 4U 0142+61 using an extraction radius of 8$'$ for both the LECS and MECS. Background subtraction was performed using standard blank field exposures. The average background subtracted source count rates are reported in Table 1 for the four observations, together with the off–axis angle and number of working MECS. The PHA spectra were rebinned so as to have $>$40 counts in each energy bin and reliably adopt a minimum χ^2 technique for model fitting. All the bins which were consistent with zero after background subtraction were rejected. Moreover the MECS spectra were restricted to the 1.8–10 keV range. Data from observation B and C were not used for spectral analysis purposes owing to poor statistics. A constant factor free to vary within a predetermined range was applied in the fitting to allow for known normalization differences the LECS and MECS.

In order to compare our results with previous observations, the spectra were first fit with two models: (i) an absorbed power–law, and (ii) an absorbed power–law plus blackbody (see Table 2). The power–law model gave an unsatisfactory description of the spectra with $\chi^2_\nu = \chi^2$/degrees of freedom (hereafter dof) of 1.6 (347 dof) and 1.9 (396) for observations A and D, respectively. We note that among simple single component spectral models, the power–law gives the lowest reduced χ^2; this is for a photon index Γ = 4.37±0.03 (A) and 4.55±0.03 (D; 90% confidence level uncertainties are used throughout the paper). The power–law plus blackbody model gave χ^2_ν = 1.28 (344) and 1.07

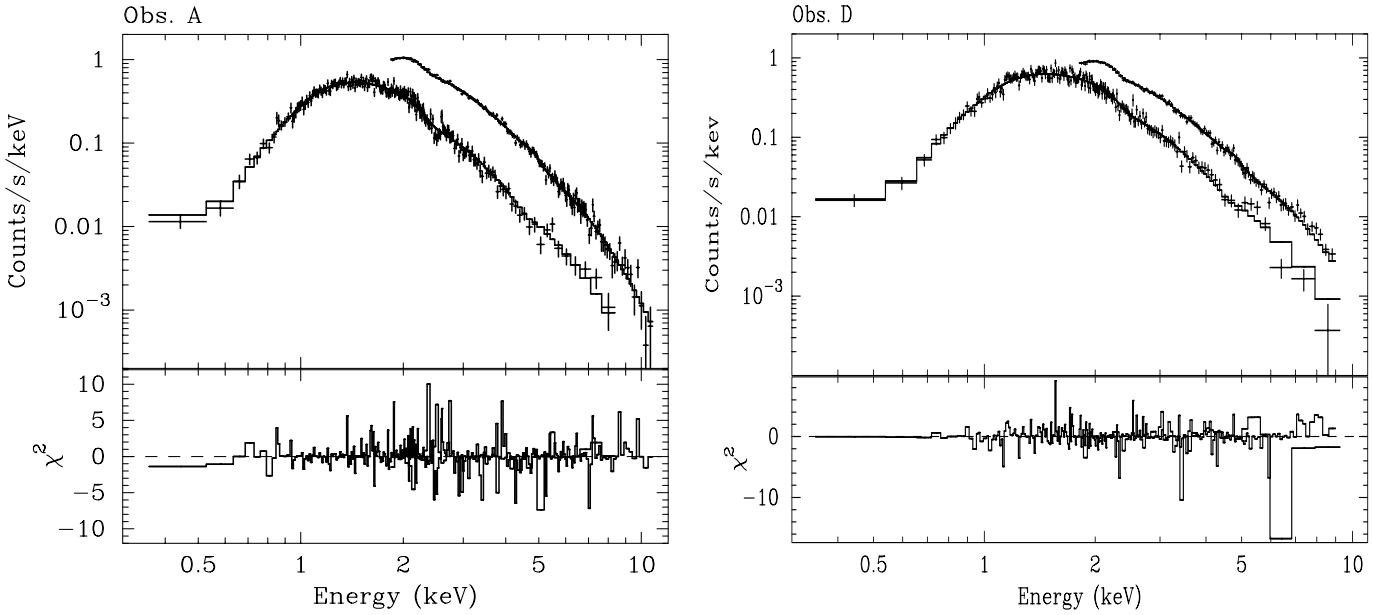

Fig. 1. LECS and MECS energy spectra of 4U 0142+61 during observation A (*left panel*) and D (*right panel*). The best fit spectral model (PL+BB; see text for details) is also shown together with the χ^2 residuals.

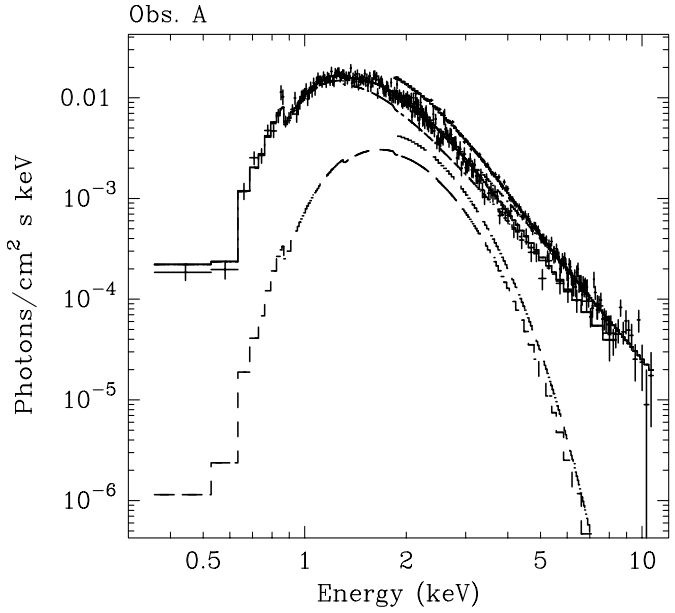

Fig. 2. 4U 0142+61 LECS and MECS unfolded spectrum for observation A. The power–law and blackbody components are shown (dotted and stepped lines).

(290) for observations A and D, respectively (see Table 2 for details).

An F–test shows that the inclusion of the blackbody component is highly significant (probability of $\sim 10^{-26}$ and $\sim 10^{-32}$ for obs. A and D, respectively). The best fit two–component spectra are plotted in Fig. 1. In Fig. 2 the unfolded energy spectrum for observation A is shown together with the contributions of the two spectral components, the power–law and the blackbody. We also fit the LECS and MECS spectra of observation A with other two–component spectral models, such as a power–law with a cut–off (χ^2/dof = 453.2/344), two blackbodies (χ^2/dof = 503.1/344) and a broken power–law (χ^2/dof = 400.6/344). All these models gave substantially worse fits than the power–law plus blackbody model. Similar results were obtained for the spectrum of observation D. Since the blackbody peaks are close to the lower end of the MECS energy range we also checked these results by analysing the LECS data only (which cover a wider spectral range than the MECS;see Table 2 and Discussion).

We also checked the stability of the results obtained by rebinning by a factor of $\sim$3 the PHA channels in the LECS and MECS spectra. Again all the bins which were consistent with zero after background subtraction were rejected from the analysis. No significant variation in the spectral parameters and uncertainties were found for either models.

The data from the High Pressure Gas Scintillation Proportional Counter (HPGSPC) and the Phoswich Detector System (PDS) did not hold any useful information on 4U 0142+61. In fact, due to the large FOVs of these intruments and the steep spectrum of 4U 0142+61, the counts above 10 keV were likely dominated by the nearby source RX J0146.9+6121.

2.2. Pulse timing, folded light curves and phase resolved spectroscopy

The arrival times of the 0.5–10 keV photons from 4U 0142+61 were corrected to the barycenter of the solar system and 1 s binned light curves accumulated for each observation. The average count rates are reported in Table 1.

The MECS counts were used to determine the 4U 0142+61 pulse period. The data from observations A, B and D were divided into 6, 4, and 5 time intervals, respectively and for each

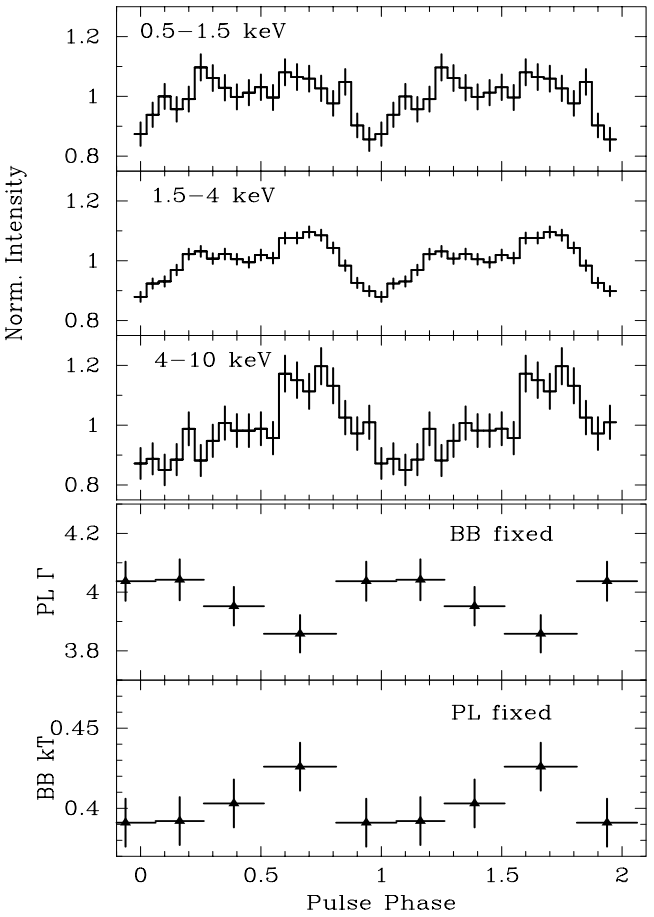

Fig. 3. The 4U 0142+61 MECS light curves for obs. A (first three panels) folded to the best period (P=8.68804 s) in the 0.5–1.5 keV, 1.5–4 keV and 4–10 keV energy bands. Zero phase was (arbitrarily) chosen to correspond to the minimum in the 1.5–4 keV folded light curve. The results of the pulse phase spectroscopy of obs. A (last two panels) are also reported for two spectral parameters. For clarity two pulse cycles are shown.

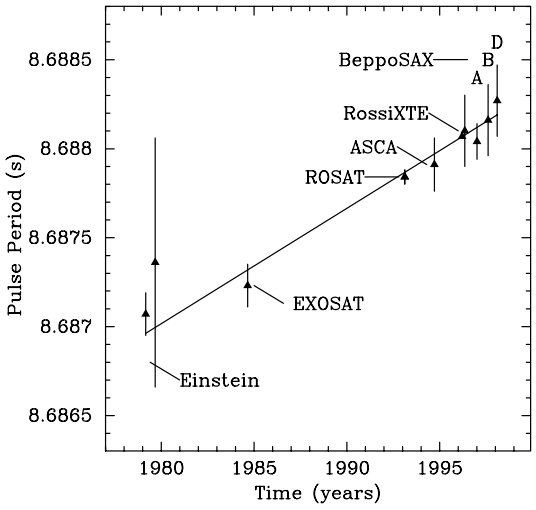

Fig. 4. Pulse period history of 4U 0142+61 as a function of time. 1σ uncertainties have been used.

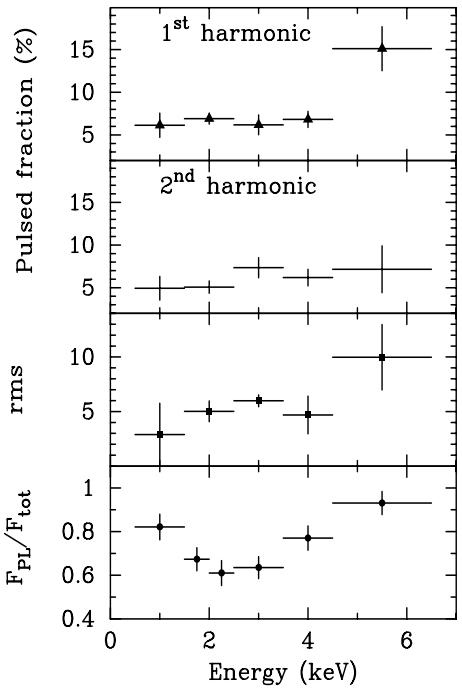

Fig. 5. Pulsed fraction of the first two harmonics of 4U 0142+61 as a function of the energy for observation A (*upper two panels*), together with the rms and the power–law to total flux ratio (*lower two panels*). See text for details.

interval the relative phase of the pulsations was determined. These phases were then fit with a linear function giving a best–fit period of 8.68804 ± 0.00007 s for observation A (see Table 3). For observation B a period of 8.6882 ± 0.0002 s was obtained, while during observation C pulsations were not detected owing to poor statistics ($\sim$ 11000 photons) to detect such a weak ($\sim$6% pulsed fraction) signal. Finally for observations D we determined a period of 8.6883$\pm$0.0001 s. The *Beppo*SAX pulse period values are plotted in Fig. 4 together with the previous measurements (see Sect. 3 for the RXTE measurement). The background subtracted light curves from observation A, folded at the best period in different energy ranges (Fig. 3; first three panels) show a double–peaked profile (see also White et al. 1996). The pulsed fraction (semiamplitude of modulation divided by the mean source count rate) was 7.1$\pm$1.5%, 7.5$\pm$0.5% and 13$\pm$2% in the 0.5–1.5 keV, 1.5–4.0 keV and 4.0–10 keV energy bands, respectively. Similar results are obtained for observations B and D.

Flux variations on several timescales are usually displayed by high accretion rate X-ray pulsars; we found no short or long–term variations in any of the *Beppo*SAX accumulated light curves.

The upper two panels of Fig. 5 show the pulsed fraction versus energy during observation A for the first two harmonics. These values were obtained by fitting the corrisponding light curves with two sinusoidal functions. The first harmonic shows a nearly constant value ($\sim$ 6%) up to 4 keV, while at higher energies increases to about 15%. A constant value of 5–7% is

Table 3. Period history for 4U 0142+61. 90% uncertainties are reported.

Mission	Instrument	Period (s)	Date (year)	Reference
Einstein	SSS	8.68707±0.00012	1979.16	(1)
Einstein	MPC	8.68736±0.0007	1979.67	(1)
it EXOSAT	ME	8.68723±0.00004	1984.66	(2)
ROSAT	PSPC	8.68784±0.00004	1993.12	(3)
ASCA	GIS	8.68791±0.00015	1994.72	(1)
RXTE	PCA	8.6881±0.0002	1996.32	(4)
RXTE	PCA	8.688068±0.000002	1996.24	(5)
*Beppo*SAX	MECS	8.68804±0.00007	1997.01	(4)
*Beppo*SAX	MECS	8.6882±0.0002	1997.61	(4)
*Beppo*SAX	MECS	8.6883±0.0001	1998.10	(4)

References: (1) White et al. 1996; (2) Israel et al. 1994; (3) Hellier 1994; (4) this work; (5) Wilson et al. 1998

inferred for the second harmonic. We calculated also the root mean square variability (rms; defined as $\sqrt{V_{obs} - V_{exp}}$ devided by the mean source count rate, where V_{obs} and V_{exp} are the observed and expected variance, respectively) of the folded light curve at different energies (third panel). Finally the ratio between the power–law and the total flux for the blackbody plus power–law spectral model is shown (lowest panel). From the comparison of these quantites we can infer that: (i) since the rms variability of the folded light curves is $\pi^{-1/2}$ times the geometric sum of the amplitudes in all available harmonics (mainly the 1^{st} and 2^{nd} in the present case), it is apparent that the behaviour is consistent with the derived amplitudes of the 1^{st} and 2^{nd} harmonics; (ii) there is evidence for an increase of the pulsed fraction ($\sim 2\sigma$ confidence level) at energies above 5 keV; (iii) there is not a simple relationship between the pulsed fraction and the flux in either of the two spectral component adopted in our analysis.

A set of four phase–resolved spectra (phase boundaries 0.06, 0.26, 0.5, 0.78) were accumulated for observation A (i.e. the observation with the highest number of source counts). These were then fit with the power–law plus blackbody model described in Sect. 2.1, with N_H fixed at the phase–averaged best–fit value. Initially, the blackbody temperature was fixed at its phase–averaged best–fit value and only the power–law parameters and blackbody normalisation were allowed to vary. The fits were then repeated with Γ fixed and blackbody parameters and power–law normalisation free (see Fig. 3). No significant changes were detected for Γ and kT as a function of the pulse phase. Similar results were obtained for the fluxes of the two spectral component.

3. RXTE observation

The 4U 0142+61 position was included in a RXTE observation pointed at the nearby high–mass X-ray binary pulsar RX J0146.9+6121 (from 1996 March 28 11:16:48 to 22:09:20; ∼20 ks of effective exposure time). The results presented here are based on data collected in the so called "Good Xenon" operating mode with the Proportional Counter Array (PCA, Jahoda et al. 1996). The PCA consists of 5 proportional counters operating in the 2–60 keV range, with a total effective area of approximately 7000 cm^2 and a field of view, defined by passive collimators, of $\sim 1\,\mathrm{deg}$ FWHM. The data consist of the time of arrival and the pulse height of each count. In order to minimise the contamination from RX J0146.9+6121 (a much harder spectrum X-ray pulsar), we considered only photons in the 2–4 keV energy interval. In order to reduce the background, only the counts detected in the first Xenon layer of each counter were used.

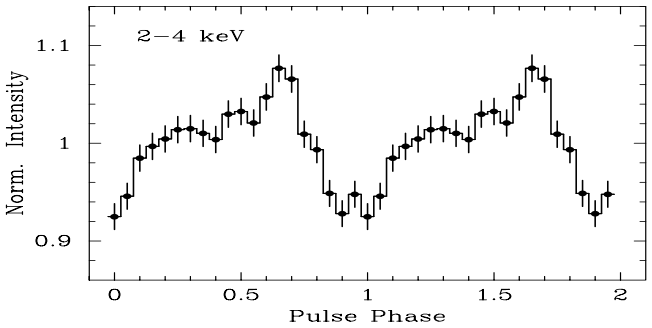

Fig. 6. The 4U 0142+61 RXTE 2–4 keV light curve folded to the best fit period (P=8.6881 s).

We obtained for 4U 0142+61 a best pulse period of 8.6881±0.0002 s (see Table 3 and Fig. 4). Fig. 6 shows the corresponding folded light curve. Despite the uncertainties in the background subtraction (the contribution from RX J0146.9+6121 is difficult to estimate), it is apparent that the RXTE/PCA pulse profile of 4U 0142+61 is similar to that observed with *Beppo*SAX. The RXTE value we obtained is consistent to within the statistical uncertainties with that of Wilson et al. (1998; energy range 3.7–9.2 keV). The somewhat different pulse shape is likely due to the different energy band used.

4. Discussion

Several models have been proposed in order to explain the nature of the "anomalous" X-ray pulsars. Mereghetti & Stella (1995) proposed that these sources form a homogeneous subclass of accreting neutron stars, perhaps members of low mass X-ray binaries (LMXBs), which are characterized by lower luminosities ($10^{35} - 10^{36}$ erg s^{-1}) and higher magnetic fields ($B \sim 10^{11}$ G) than classical LMXBs. However the lack of evidence for a binary nature from any of these systems (Mereghetti et al. 1998; Wilson et al. 1998) argues in favor of models in which the X-ray emission originates from a compact object that is not in an interacting binary system.

Van Paradijs et al. (1995) proposed that AXPs are young population I objects, which originate from the evolution of short orbital period High Mass X-ray Binaries (HMXBs), following the expansion of the massive star and the onset of unstable Roche Lobe overflow, before central hydrogen is exhausted (see also Cannon et al. 1992). The resulting common–envelope phase should cause the neutron star to spiral–in and disrupt the com-

panion star after the so–called Thorne–Żytkov stage. Therefore, these sources should consist of an isolated neutron star accreting matter from a residual disk with a mass in the $10^{-3} - 1\,M_{\odot}$ range. The blackbody component in 4U 0142+61 and, likewise, other AXPs has been interpreted as evidence for quasi–spherical accretion onto an isolated neutron star formed after common envelope and spiral–in of a massive short–period ($P_{orb} \leq 1$ yr) X-ray binary. In this case the remains of the envelope of the massive star might produce two different types of matter inflow: a spherical accretion component with low specific angular momentum giving rise to the blackbody component and a high specific angular momentum component which forms an accretion disk and is likely responsible for the power–law emission (Ghosh et al. 1997). Although some problems remain open in this scenario, we note that a post common–envelope evolutionary scenario for 4U0142+614 is also suggested by the inference that about half of the X-ray absorbing material is close to the source (White et al. 1996). In this context it is interesting to note that independent evidence supports the view that the binary X-ray pulsars 4U1626–67 and HD49798 were formed following a common envelope and spiral–in evolutionary phase (see Angelini et al. 1995 and Israel et al. 1997 and references therein). The different properties of the companion stars in these two cases may reflect the fact that unstable mass transfer set in at different evolutionary phases in the nuclear evolution of their progenitors (in turn, reflecting different initial masses and orbital periods; see also Ghosh et al. 1997).

Thompson & Duncan (1993, 1996) proposed that the AXPs are "magnetars", neutron stars with a superstrong magnetic field ($\sim 10^{14-15}$ G). This proposal is supported by the similarity in the pulse periods (8.05 , 7.5 s and 5.16 s) and of $\dot{P}$ values measured in the Soft γ–ray Repeaters SGR0520–66, SGR1806-20 and SGR1900+14, respectively (Kouveliotou et al. 1998; Hurley et al. 1998). If this connection proved correct, AXPs, would be quiescent soft γ–ray repeaters. Heyl & Hernquist (1997) argued that their emission may be powered by the cooling of the core through a strongly magnetised envelope of matter (made up mainly by hydrogen and helium). Pulsations would originate from a temperature gradient on the surface of the star. Moreover Heyl & Hernquist (1998) showed that in this scenario, spin–down irregularities, observed in the period history of two "anomalous" X-ray pulsars (1E 2259+58 and 1E 1048–59), may be simply accounted for with glitches like those observed in young radio pulsars.

The 0.5–10 keV spectrum of 4U 0142+61 is well modelled by the sum of an absorbed steep power–law and a low–energy blackbody. The latter component was introduced by White et al. (1996) based on the ASCA data; the corresponding blackbody radius and flux were $\sim 2.4 \pm 0.3$ km (at 1 kpc) and $\sim$40% of the total, respectively. Neither the power–law photon index nor the blackbody temperature show evidence of changes across different *Beppo*SAX observations. We found marginal evidence (at about 2σ confidence level) for changes relative to previous observations. A comparison of the ASCA and *Beppo*SAX results show that: (i) the power–law photon index increases by about 4% (observations A and D); (ii) the blackbody radius decreased by about 37% (A) and 12% (D); (iii) the blackbody flux decreased to $\sim$30% (A) and $\sim$35% (D) of the total flux therefore showing a $\sim$10%–5% decrease with respect to that of the ASCA observation; (iv) the 0.5–10 keV total flux decreased of about 15–12%.

By fixing the parameters N_H, kT and Γ to the values inferred by ASCA, the *Beppo*SAX observation A spectrum gives a χ^2_ν/dof of 1.9/348. In this case the blackbody component accounts for $\sim$30% of the total flux ($\sim$10% lower than that of ASCA). As an additional test we also merged the data for observation A (MECS 2 and 3 only) and D and fit them with the power–law plus blackbody model (see Table 2). While a small change in the spectral parameters is found relative to observations A and D, separately, the blackbody flux is $\sim$30% of the total.

To remove possible effects introduced by the vicinity of the lower end of the energy range of the MECS and the peak of the blackbody component, we also fitted the spectrum of observations A, D and A+D by using only the data as accumulated by the LECS, the energy band of which uninterruptely covers the range 0.5–9.0 keV and allows a better fit in the energy interval (1–4 keV) where the power–law and the blackbody components overlap. Again we obtained results similar to the LECS+MECS case, but with a larger uncertainty. All these results point to a marginal variation of the spectral parameters of 4U 0142+61, if any.

The *Beppo*SAX data suggest that the pulsed fraction for energies above 4 keV decreased (from 25%$\pm$5% with ASCA to 13%$\pm$2% with *Beppo*SAX; 90% uncertainties). For these energies the counts are almost entirely dominated by the power–law component (in the spectral model assumed).

The pulse periods measured by *Beppo*SAX show that 4U 0142+61 has continued its secular spin–down during 1996–1998 (see Fig. 4). The period derivative inferred from the *Beppo*SAX observations alone ($\sim 6.0 \pm^{7}_{5.1} \times 10^{-12}$ s s^{-1}) is consistent with the average spin–down rate ($\sim 2 \times 10^{-12}$ s s^{-1}) inferred over the 19 yr span of the historical dataset (note that in the period list we did not include the low significance detections inferred on 1985 November 11 and December 11 with EXOSAT ME, and on 1991 February 13 with ROSAT HRI; Israel et al. 1994). The inferred $\dot{P}$ for 4U 0142+61 is consistent with the uncertainties of all pulse period measurements except, perhaps, one (the 1979 *Einstein* SSS one; see Fig. 4) implying that, so far, no "glitches" have been observed yet.

Acknowledgements. We would like to thank Giancarlo Cusumano for providing the MECS off–axis matrices and the *Beppo*SAX Mission Planning for their constant help. The authors also thank K. Long the comment of which helped to improve an earlier version of this paper. This work was partially supported through ASI grants.

References

Angelini L., White, N.E., Nagase F., et al., 1995, ApJ 449, L41
Boella G., Chiappetti L., Conti G., et al., 1997, A&AS 122, 327
Cannon R.C., Eggleton P.P., Żytkov A.N., et al., 1992, ApJ 386, 206
Coe M.J., Pightling S.L., 1998, MNRAS 299, 223

Corbet R.H.D., Smale A.P., Ozaki M., Koyama K., Iwasawa K., 1995, ApJ 443, 786
Ghosh P., Angelini L., White N.E., 1997, ApJ 478, 713
Gotthelf E.V., Vasisht G., 1998, New Astronomy 3, 293
Hellier C., 1994, MNRAS 271, L21
Heyl J.S., Hernquist L., 1997, ApJ 489, L67
Heyl J.S., Hernquist L., 1998, ApJ 506, L61
Hurley K., Kouveliotou C., Murakami T., et al., 1998, IAU Circ. 7001
Israel G.L., Mereghetti S., Stella L., 1994, ApJ 433, L25
Israel G.L., Stella L., Angelini L., et al., 1997, ApJ 474, L53
Jahoda K., Swank J. H., Giles A. B., et al., 1996, SPIE 2808, 59
Kouveliotou C., Dieters, S., Strohmayer T., et al., 1998, Nat 393, 235
Mereghetti S., Stella L., 1995, ApJ 442, L17
Mereghetti S., Stella L., De Nile F., 1993, A&A 278, L23
Mereghetti S., Israel G.L., Stella L., 1998, MNRAS 296, 689
Motch C., Belloni T., Buckley D., et al., 1991, A&A 246, L24
Oosterbroek T., Parmar A.N., Mereghetti S., Israel G.L., 1998, A&A 334, 925
Parmar A.N., Martin D.D.E., Bavdaz M., et al., 1997, A&AS 122, 309
Parmar A.N., Oosterbroek T., Favata F., et al., 1998, A&A 330, 175
Steinle H., Pietsch W., Gottwald M., Graser U., 1987, Ap&SS 131, 687
Sugizaki M., Nagase F., Torii K., et al., 1997, PASJ 49, L25
Thompson C., Duncan R.C., 1993, ApJ 408, 194
Thompson C., Duncan R.C., 1996, ApJ 473, 322
Torii K., Kinugasa K., Katayama K., et al., 1998, ApJ 503, 843
Van Paradijs J., Taam R.E., van den Heuvel E.P.J., 1995, A&A 299, L41
Vasisht G., Gotthelf E.V., 1997, ApJ 486, L129
Wilson C.A., Dieters S., Finger M., et al., 1998, ApJ 513, 464
White N.E., Mason K.O., Giommi P., et al., 1987, MNRAS 226, 645
White N.E., Angelini L., Ebisawa K., et al., 1996, ApJ 463, L83